https://doi.org/10.5194/egusphere-2023-610
Preprint. Discussion started: 25 April 2023

F-region drift current distribution by X wave ionospheric heating

Yong Li [1,2], Hui Li[2], Jian Wu[1,2], Xingbao Lv [1,3,4], Chengxun Yuan[1,3,4] , Ce Li[1], Zhongxiang Zhou[1,3,4]

[1] School of Physics, Harbin Institute of Technology, Harbin 150001, China
[2] China Research Institute of Radio Wave Propagation, Beijing 102206, China
[3] Heilongjiang Provincial Key Laboratory of Plasma Physics and Application Technology, Harbin 150001, China
[4] Heilongjiang Provincial Innovation Research Center for Plasma Physics and Application Technology, Harbin 150001, China

Correspondence to: Hui Li(lihui_2253@163.com); Zhongxiang Zhou(zhouzx@hit.edu.cn)

Abstract. We present a theoretical and numerical study of drift current model in the ionosphere by incorporating the ohmic heating model and the magnetohydrodynamic (MHD) momentum equation. Based on these equations, the ionospheric electron temperature and drift current are investigated. The results indicate that the maximum change of electron temperature ΔT_e is about 570 K, and the ratio is $\Delta T_e / T_e \sim 48\%$. The maximum drift current density is $8\times10^{-10}\,\mathrm{A}\cdot m^{-2}$, and its surface integral is 5.76 A. Diamagnetic drift current is the main form of current. The low collision frequency between charged particles and neutral particles has little effect on the current, and the collision frequency of electrons and ions is independent of the drift current. The current density profile is a flow ring. We present the effective conductivity as a function of the angle between the geomagnetic field and the radio wave; the model explains why the radiation efficiency in Kotik's experiment was strongest when the X wave is heating along the magnetic dip angle.

1 Introduction

Extremely low frequency (ELF) waves have irreplaceable advantages in communication, navigation, and magnetospheric studies. In the 1970s, Willis and Davis first proposed the theory of modulating ionospheric excited ELF waves(Willis and Davis, 1973). Then Getmantsev et al. successfully excited ELF signals in experiments(Getmantsev et al., 1974).

There are several main physical mechanisms of ELF signal excitation through modulated heating of the ionosphere. The first mechanism is called the polar electrojet model (PEJ). A polar electrojet is a strong horizontal electric current driven by an atmospheric dynamo electric field and magnetospheric electric field. It can be effectively modulated by heating the ionosphere with modulated high-frequency (HF) wave. The resulting modification of the electrojet current creates an effective antenna radiating at the modulation frequency(Stubbe et al., 1981; Stubbe and Kopka, 1977; Rietveld et al., 1987). Numerous researchers have analyzed this process theoretically and experimentally, and have proposed optimization measures such as preheating(Milikh and Papadopoulos, 2007), geometric modulation(Cohen et al., 2008, 2009), and beam painting(Papadopoulos et al., 1990) to enhance the radiation signal. The shortcoming of PEJ is that the current changes suddenly and is difficult to predict(Belyaev et al., 1987). Beat-wave (BW) modulation can also excite ELF waves by dividing the heating source into two groups(Ganguly, 1986; Kuo et al., 2012), in which one group transmits a continuous wave at a frequency f_0, and the other group transmits a continuous wave at a frequency $f_0 \pm f$ (f is the ELF/VLF modulation frequency).

Barr et al. suggested that the heating occurs in the D layer and is equivalent to the beat-wave AM mode(Barr and Stubbe, 1997), but Kuo et al. proposed that the heating occurs in the F layer and is driven by the ponderomotive force(Kuo et al., 2010; Kuo et al., 2011). It is still controversial where the source region of ELF/VLF waves generated by BW modulation is located.

In 2011, Papadopoulos proposed an ionospheric current drive (ICD) model based on the experimental results of the High Frequency Active Auroral Research Program (HAARP)(Papadopoulos et al., 2011a). The idea is that HF heating creates a pressure gradient in the heated region, leading to a diamagnetic current that excites a hydromagnetic wave with the modulation frequency. Kotik et al. verified the mechanism experimentally in SURA, and discussed the effects of HF emission frequency, emission direction, and magnetic field activity on radiation signals(Kotik et al., 2015; Kotik et al., 2013). Theoretically, Papadopoulos proposed that ELF currents are driven in a two-step process based on the model of Lysak(Papadopoulos et al., 2011b; Lysak, 1997). Eliasson et al. established the propagation model of ELF waves in the polar region based on the Hall MHD model(Eliasson et al., 2012), and Sharma established the radiation propagation model in the mid and low latitudes on this basis(Sharma et al., 2016).

At present, theoretical research on ICD theory focuses mainly on the propagation process of ELF wave. Eliasson and Sharma discuss mainly the impact of collisions and magnetic fields on wave propagation; in their papers, the current source is given by an empirical formula. The effect of HF heating on current distribution has not been studied in previous reports. In this paper, we develop the ionospheric drift current model by coupling the ohmic heating equation and MHD momentum equation. We then study the drift-current properties and the effects of collisions and transmitter angle on the drift current.

This paper is organized as follows: In Section 2, we give the ohmic heating model for tensor conductivity and derive a formula for ionospheric drift current using the MHD momentum equation. In Section 3, numerical solutions of the model are presented for realistic ionospheric profiles, drift current properties are discussed, and the effect of emission angle is analyzed. Finally, in Section 4, the conclusions are presented.

2 Theoretical model

2.1 HF heating model

Background ionospheric data used in this work are obtained from HAARP; the magnetic field inclination is assumed to be 90°. The heating model is simplified into a two-dimensional plane, in which the z axis is parallel to the geomagnetic field, and x axis is perpendicular to the magnetic field. The ohmic heating equation is (Shoucri et al., 1984; Lofas et al., 2009)

$$\frac{3}{2}k_B N_e \frac{\partial T_e}{\partial t} = \nabla\bullet(\overline{\overline{K_e}}\bullet\nabla T_e) + Q_{HF} + Q_0 - L_e(T_e,T_0) \qquad (1)$$

where k_B is Boltzmann's constant, N_e is electron density, T_e is electron temperature, Q_0 is the background power source, Q_{HF} is ohmic heating by high-power radio waves, $L_e(T_e,T_0)$ is the rate of energy loss due to both elastic and inelastic collisions with ions and neutral particles, and $\overline{\overline{K_e}}$ is the thermal conductivity tensor, which come from Banks(Kockarts, 1973)

$$\overline{\overline{K_e}} = \begin{pmatrix} 0 & 0 & 0 \\ 0 & 0 & 0 \\ 0 & 0 & K_{e0} \end{pmatrix} \tag{2}$$

$$K_{e0} = \frac{7.7\times10^{5} T_e^{5/2}}{1+3.22\times10^{4}(T_e^{2}/N_e)\sum_n N_n Q_D} \tag{3}$$

Here N_n is the density of neutral particles of species *n*, and Q_D is the average momentum transfer cross-section, which is calculated by Schunk and Nagy(Schunk and Nagy, 2009). Q_{HF} is calculated from the ordinary expression for Joule heating,

$$Q_{HF} = \frac{1}{2}\mathrm{Re}\left[\mathbf{E}^{*}\bullet\overline{\overline{\sigma}}\bullet\mathbf{E}\right] \tag{4}$$

where $\overline{\overline{\sigma}}$ is the conductivity tensor(Gurevich, 2012)

$$\overline{\overline{\sigma}} = \begin{pmatrix} \sigma_{xx} & \sigma_{xy} & \sigma_{xz} \\ \sigma_{yx} & \sigma_{yy} & \sigma_{yz} \\ \sigma_{zx} & \sigma_{zy} & \sigma_{zz} \end{pmatrix} \tag{5}$$

$$\begin{aligned}
\sigma_{xx} &= \sigma_{yy} = \frac{\varepsilon_0 \omega_{pe}^2 v_e}{2}\left[\frac{1}{(\omega-\omega_{ce})^2+v_e^2}+\frac{1}{(\omega+\omega_{ce})^2+v_e^2}\right] \\
\sigma_{xy} &= -\sigma_{yx} = -i\frac{\varepsilon_0 \omega_{pe}^2 v_e}{2}\left[\frac{1}{(\omega-\omega_{ce})^2+v_e^2}-\frac{1}{(\omega+\omega_{ce})^2+v_e^2}\right] \\
\sigma_{zz} &= \frac{\varepsilon_0 \omega_{pe}^2 v_e}{\omega^2+v_e^2} \\
\sigma_{xz} &= \sigma_{zx} = \sigma_{yz} = \sigma_{zy} = 0
\end{aligned} \tag{6}$$

Here ε_0 is the vacuum dielectric constant; $\omega, \omega_{pe}, \omega_{pe}, v_e$ are, respectively, the frequency of the incident wave, the ionospheric frequency, the cyclotron frequency, and the frequency of electron collision with other particles; **E** is the incident electric field; and the incident wave is generally an X wave or O wave

$$\begin{aligned}
\mathbf{E}_{\mathrm{X}} &= E_0(s)\sin(\theta)x + \mathrm{i}E_0(s)y + E_0(s)\cos(\theta)\hat{z} \qquad \text{X wave} \\
\mathbf{E}_{\mathrm{O}} &= E_0(s)\sin(\theta)x - \mathrm{i}E_0(s)y + E_0(s)\cos(\theta)\hat{z} \qquad \text{O wave}
\end{aligned} \tag{7}$$

where θ is the angle between the incident wave and the z-axis and $E_0(s)$ is the electric field intensity in the ionosphere(Gustavsson et al., 2010)

$$E_0(s)=E(s_0)\left(\frac{s_0}{s}\right)\left[\frac{\varepsilon(s_0)}{\varepsilon(s)}\right]^{0.25}\exp\left(ik_0\int_{s_0}^{s}N(s)ds\right) \tag{8}$$

where s is the coordinate along the propagation direction of the wave, $\varepsilon(s)$ is the relative dielectric constant, $N(s)$ is the refractive index of the wave in the ionosphere, and the electric field amplitude $E(s_0)$ is estimated by an empirical formula,

$$E(s_0)=\frac{\sqrt{30ERP}}{s_0} \tag{9}$$

where ERP is the effective radiated power of the transmitter. $L_e(T_e,T_0)$ is the electron cooling rate, which depends mainly on the elastic electron-ion collisions, the elastic electron–neutral collisions, the rotational and vibrational excitation of N_2 and O_2, and the fine structure excitation of O(Moore, 2007).

2.2 Ionospheric drift current model

There is no drift current in the direction of the magnetic field because of the electric neutrality in ionosphere(Chen, 2012). We consider mainly the current induced perpendicular to the magnetic field and ignore the current parallel to the field. In order to simplify the calculation, the positive ion is set as a single O^+ ion, and the collision between electrons and ions ν_{ei}, electrons and neutral particles ν_{en}, and ions and neutral particle ν_{in} are considered. The influence of neutral wind is ignored. The MHD momentum equation can be written

$$m\frac{d\mathbf{V}_{e\perp}}{dt}=-e\mathbf{E}-e\mathbf{V}_{e\perp}\times\mathbf{B}-\frac{\nabla_\perp P_e}{N_e}-m\nu_{en}\mathbf{V}_{e\perp}-\mathrm{m}\nu_{ei}(\mathbf{V}_{e\perp}-\mathbf{V}_{i\perp}) \tag{10}$$

$$M\frac{d\mathbf{V}_{i\perp}}{dt}=e\mathbf{E}+e\mathbf{V}_{i\perp}\times\mathbf{B}-M\nu_{in}\mathbf{V}_{i\perp}+\mathrm{m}\nu_{ei}(\mathbf{V}_{e\perp}-\mathbf{V}_{i\perp}) \tag{11}$$

In this work, we focus on the steady state. Therefore, the left sides of Eqs. (10) and (11) are ignored. the electric force can also be ignored since this paper focuses on low frequency variations. The current can be expressed as

$$J_\perp=N_e e(\mathbf{V}_{i\perp}-\mathbf{V}_{e\perp}) \tag{12}$$

Solving Eq. (10), (11), and (12), we get

$$J_x=e\frac{\nabla_\perp P_e\left(m\nu_{en}+M\nu_{in}\right)\left(M\nu_{ei}\nu_{in}+m\omega_{ce}^2\right)}{m(\nu_{ei}{}^2\left(m\nu_{en}+M\nu_{in}\right)^2+m\left(m\nu_{en}\left(2\nu_{ei}+\nu_{en}\right)+2M\nu_{ei}\nu_{in}\right)\omega_{ce}^2+m^2\omega_{ce}^4)} \tag{13}$$

$$J_y = -e\frac{\nabla_\perp P_e \omega_{ce}\left(M(\nu_{ei}-\nu_{en})\nu_{in} + m(\nu_{in}\nu_{en}+\omega_{ce}^2)\right)}{\nu_{ei}^2(m\nu_{en}+M\nu_{in})^2 + m(m\nu_{en}(2\nu_{ei}+\nu_{en})+2M\nu_{ei}\nu_{in})\omega_{ce}^2 + m^2\omega_{ce}^4} \tag{14}$$

where

$$\begin{aligned}\nu_{en} = {} & 2.33\times10^{-17} N_{N_2}(1-1.21\times10^{-4}T_e)T_e + 2.65\times10^{-16} N_O T_e^{0.5} \\ & +1.82\times10^{-16} N_{O_2}(1+0.036T_e^{0.5})T_e^{0.5}\end{aligned} \tag{15}$$

$$\nu_{ei} = 5.4\times10^{-5} N_e / T_e^{1.5} \tag{16}$$

$$\begin{aligned}\nu_{in} = {} & 6.64\times10^{-16} n(\mathrm{O_2}) + 3.67\times10^{-17} n(\mathrm{O}) T_i^{0.5}[1-0.064\log10(T_i)]^2 \\ & +6.82\times10^{-16} n(\mathrm{N_2})\end{aligned} \tag{17}$$

Coupling with the ohmic heating model of the ionosphere, the spatial distribution of electron pressure can be obtained. The spatial distribution of drift current can then be obtained by substituting pressure into Eq. (13) and (14).

3 Simulation results and discussion

In this section, we analyze the drift current caused by ohmic heating according to the theoretical model developed in the preceding section. Background data were acquired at HAARP on 2 October 2011. The ionospheric and atmospheric background profiles are given by the International Reference Ionosphere (IRI-2016) model and the neutral atmosphere model (MSIS), as well as geomagnetic field data from the IGRF model. Figure 1 shows the background data. The critical frequency of the ionosphere is 3.67 MHz and its altitude is 350 km.

The computational domain is –150 to 300 km in the x-axis direction, and 150 to 450 km in the z-axis direction, and the spatial grid size is 2 km. The ERP of the transmitter is set at 500 MW; the transmitting frequency is set at 4 MHz, which is greater than the ionospheric critical frequency; the transmitting half-width of the transmitter is set at 7°; and the transmitting waveform is an X wave.

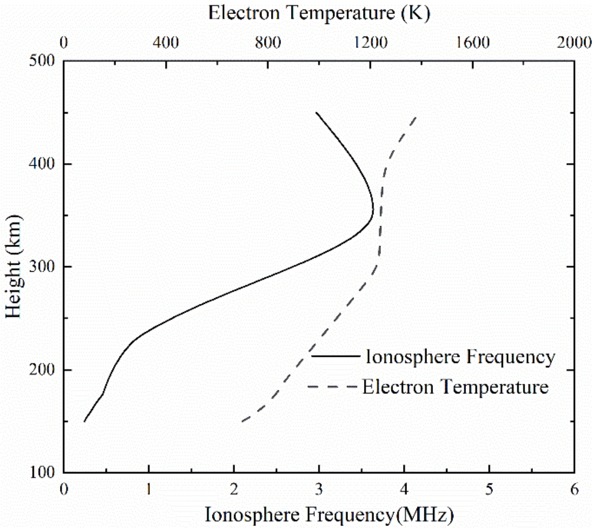

Figure 1. Background ionospheric electron frequency and electron temperature.

3.1 Ionospheric heating effect and drift current

Figure 2 shows the change in the ionosphere after the heating is stable when $\theta = 0$. Figure 2(a) shows that the maximum temperature change is $\Delta T_e \sim 570$ K when heating is stable, and the change ratio is $\Delta T_e / T_e \sim 48\%$. The corresponding electron pressure is given in Fig. 2(b); it is about 4.1×10^{-9} Pa in the center of the heated area. According to the pressure changes obtained from Fig. 2(b), the ionosphere's current density distribution can be obtained using Eq. (15) and (16). The results are shown in Fig.2(c) and (d), the maximum value of J_y is approximately $7.8\times10^{-10}\,\mathrm{A\cdot m^{-2}}$, and J_x is approximately $9.3\times10^{-43}\,\mathrm{A\cdot m^{-2}}$. The J_y direction is along the vertical pressure gradient and J_x is along the pressure gradient.

We calculate various frequencies at the position of critical frequency and find $v_{en} = 2$ Hz, $v_{in} = 0.29$ Hz, $\omega_{ce} = 1.28$ MHz. Therefore, ignoring the collision frequency of electrons and ions with neutral particles in Eq. (13) and (14) is reasonable, and the equations can be solved to give

$$J_x \approx 0, J_y \approx -e\nabla_\perp P_e / m\omega_{ce} \tag{18}$$

This means there is no current generated in the x direction, and the current generated in the y direction is mainly diamagnetic drift current. What's interesting about this simplification is that we don't constrain the electron-ion collisions, so the electron-ion collisions don't affect the F layer drift current. When J_y is positive, the current flows inward perpendicular to the xz plane; when it is negative, the current flows outward. Therefore, the diamagnetic current is cylindrically symmetric about the z axis. The distribution of current in the horizontal plane at the critical frequency position is shown in Fig. 3 (obtained by sweeping). The arrow in the figure indicates that the direction of current flow is counterclockwise in this frame, with zero current in the heating center, gradually increasing and then decreasing towards the outside.

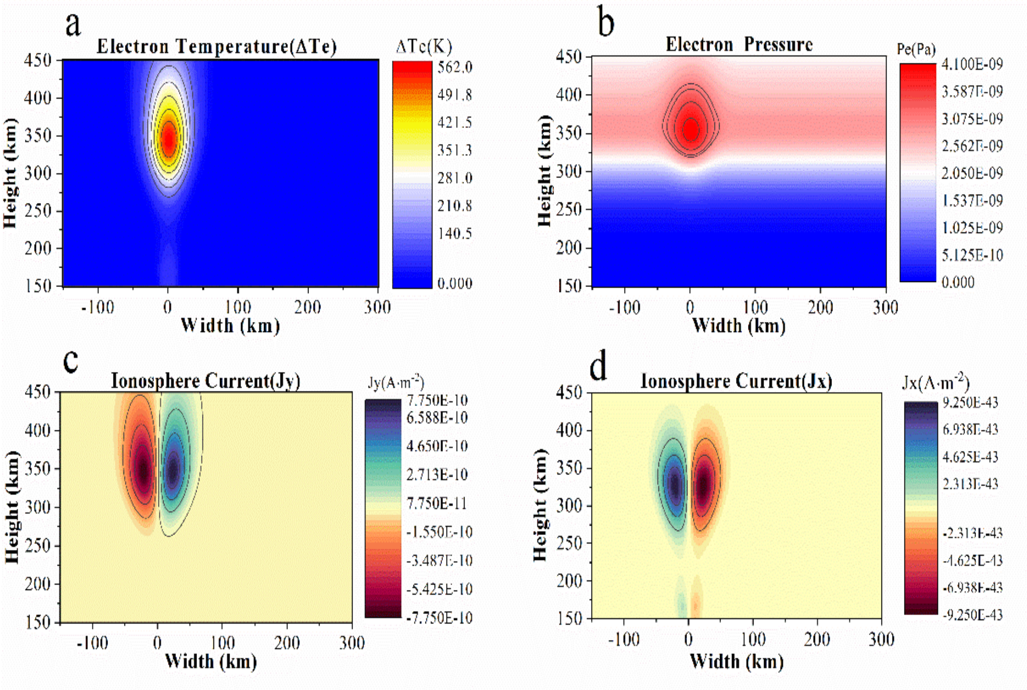

Figure 2. when the heating is stable. (a) Electron temperature. (b) Electron pressure, (c) J_y current distribution. (d) J_x current distribution.

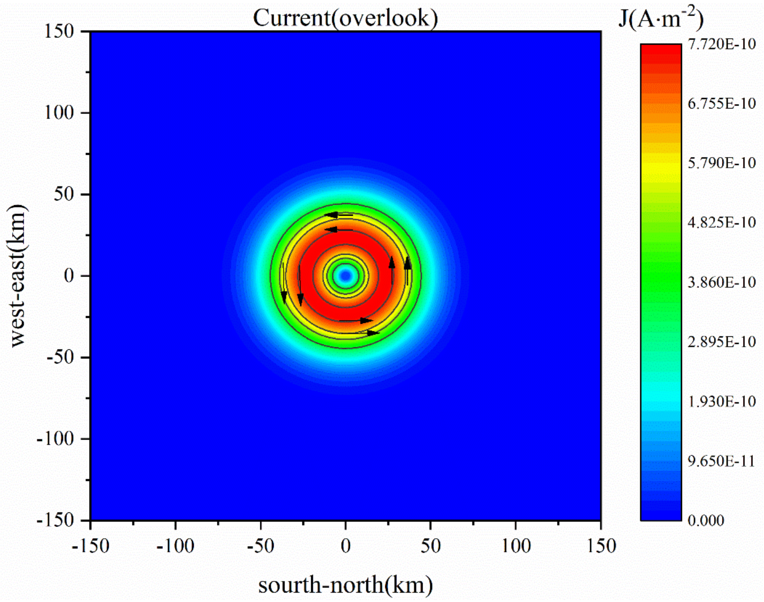

Figure 3. Horizontal distribution of drift current at the critical frequency position.

3.2 Influence of different angles on drift current

According to Kotik's experimental results, the strongest low-frequency electromagnetic signal is received on the ground when the HF wave heating direction is parallel to the magnetic field, and the radiated signal decreases as the angle between the radio wave and the geomagnetic field increases. This section provides a theoretical explanation for this observation. We study the effect of different heating directions on drift current by fixing other transmitter parameters and setting the angle $\theta = 10^{\circ}, 20^{\circ}, 30^{\circ}$. The temperature change ΔT_e and current J_y in the ionosphere are shown in Fig. 4. Figure 4(a), (c), and (e) show diagrams of electron temperature ΔT_e at $\theta = 10^{\circ}, 20^{\circ}, 30^{\circ}$ respectively. It is obvious that with an increase of θ, the heating area is shifted horizontally, and the heating effect gradually weakens. Figure 4(b), (d), and (f) show diagrams of current at $\theta = 10^{\circ}, 20^{\circ}, 30^{\circ}$. The currents undergo the same kind of change as the temperature.

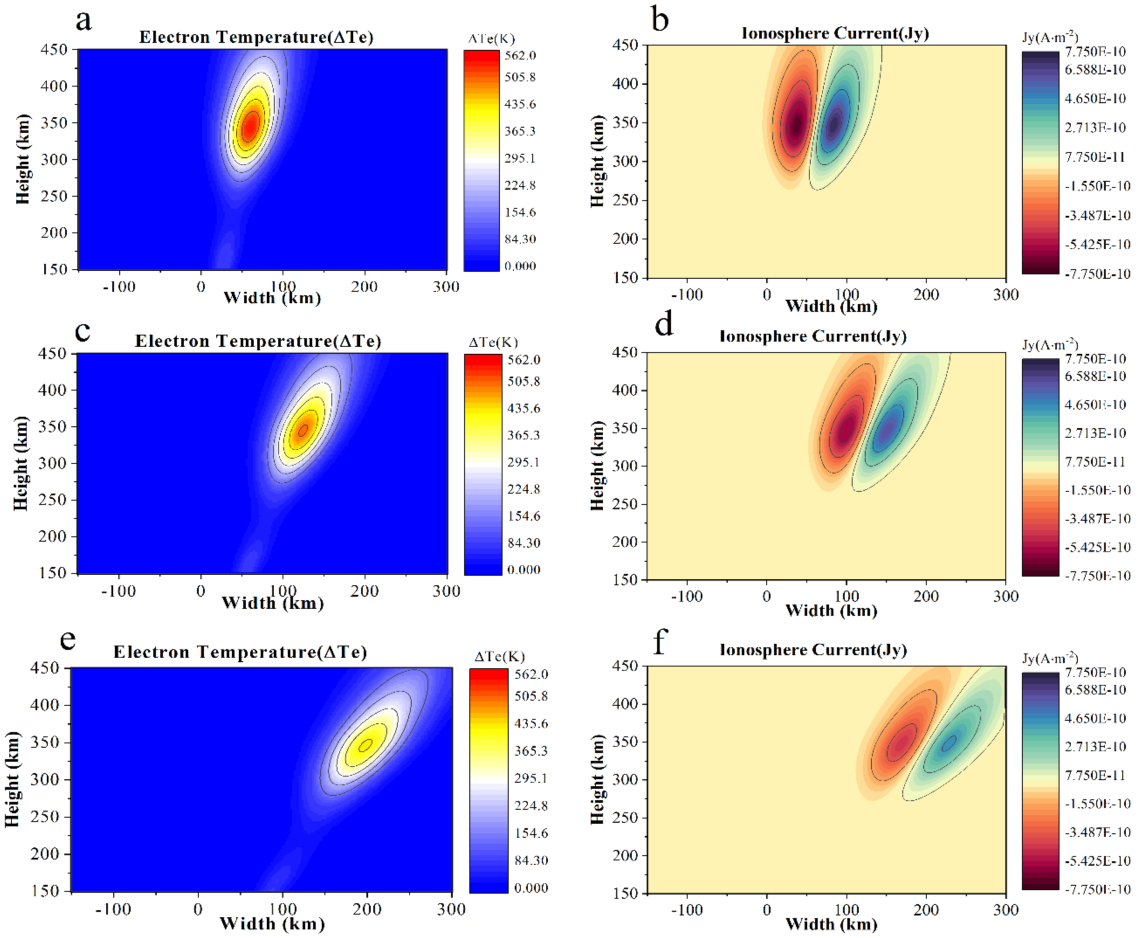

Figure 4. Distributions of (a) electron temperature at θ=10°, (b) current J_y at θ=10°, (c) electron temperature at θ= 20°, (d) current J_y at θ =20°, (e) electron temperature at θ =30°, (f) current J_y at θ =30°.

In order to see the effects of θ more visually, the maximum temperature change for different angle θ is shown by the red dots in Fig. 5. The electron temperature change is 560 K at $\theta = 0$ and is reduced to 430 K at $\theta = 30°$. We also performed a plane integration of the absolute values of the current density (avoiding positive and negative cancellation); the results are marked by the green triangles in Fig. 5. It can be seen that the current reaches 5.76 A during vertical heating and decreases gradually with increasing angle, a changing trend that matches that of the temperature.

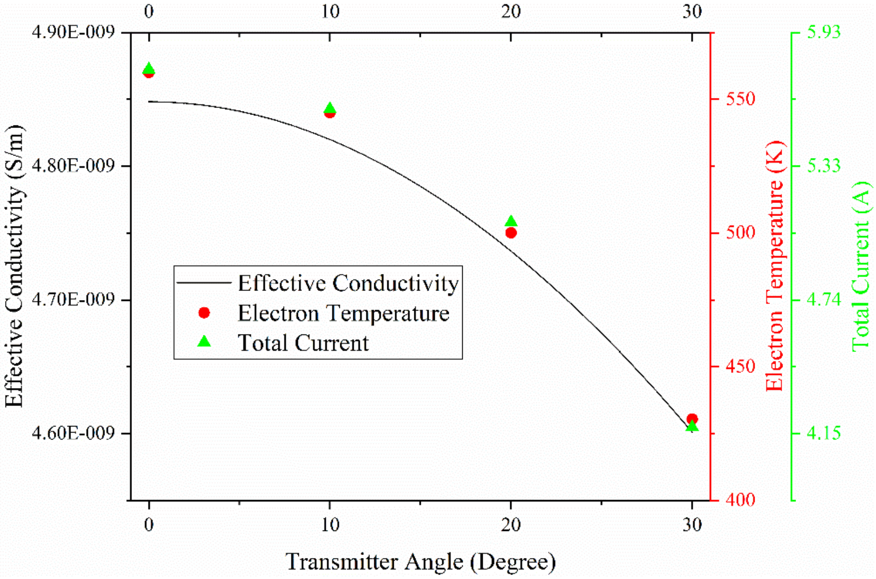

Figure 5. Effective conductivity, electron temperature, and total current as functions of angle *θ*.

To explore what causes the changes of electron temperature and current, we calculated the effective conductivity at different angles. Combining Eq. (4) and (6), the dependence of effective conductivity on angle can be derived:

$$\sigma_{ef} = \frac{\varepsilon_0 \omega_{pe}^2 v_e}{\omega^2 + v_e^2}\sin^2(\theta) + \frac{\varepsilon_0 \omega_{pe}^2 v_e}{2}\Big(\big(\frac{1}{(\omega-\omega_{ce})^2 + v_e^2} + \frac{1}{(\omega+\omega_{ce})^2 + v_e^2}\big)(1+\cos^2(\theta)) + \big(\frac{1}{(\omega-\omega_{ce})^2 + v_e^2} - \frac{1}{(\omega+\omega_{ce})^2 + v_e^2}\big)\cos(\theta)\Big) \quad (19)$$

Choosing the ionospheric Debye frequency, electron cyclotron frequency, collision frequency, and transmitter frequency at the corresponding heights, we obtain a relationship between the angle and the effective conductivity, as shown by the black line in Fig. 5. It can be seen from the graph that the effective conductivity decreases gradually as the angle θ increases. We find the trend of effective conductivity is the same as the trends exhibited by temperature and current. Physically, it is the change of effective conductivity that causes the change of heating. The conductivity is greatest when $\theta = 0$, where the heating effect is best and the current is the greatest. This could provide a natural explanation for the signal reaching its maximum values in Kotik's experiment where the beam was directed along the Earth's magnetic field(Kotik et al., 2013).

4 Conclusions

We have established a model of drift current in the ionosphere using the ohmic heating model and MHD momentum equation, and have found a formula to calculate the drift current. The following conclusions are reached based on these calculations.

1) When the ERP is 500 MW and θ = 0°, the ionospheric electron temperature change ΔT_e is about 570 K, and the change ratio $\Delta T_e / T_e \sim 48\%$. From the calculated distribution of drift current in the ionosphere, the maximum value of J_y is found to be approximately 7.8×10^{-10} A·m^{-2}, and J_x is approximately 9.3×10^{-43} A·m^{-2}. The total current excited by heating is 5.76 A.
2) It is concluded that the collisions of charged particles with neutral particles have negligible effect on the current; but electron-ion collisions do not affect the drift current. The current is mainly diamagnetic drift current and it is ring-shaped, zero at the center and gradually increasing outward until it decreases again.
3) An analytical equation of the dependence of effective conductivity σ_{ef} on emission angle θ is given. The effect of the emission angle θ on the electron temperature and current density is explained by using the concept of effective conductivity, and it is demonstrated that the strongest current is obtained along the magnetic field direction when the ionosphere is heated by X-wave, and that the current gradually decreases as the angle increases. Theoretically, this explains why the strongest signal is received by the ground when heated along the magnetic inclination angle.

Data availability

The ionospheric background parameters of our numerical simulation in this paper are from https://ccmc.gsfc.nasa.gov/ modelweb/models/iri2016 vitmo.php, and The ionospheric background parameters are from http://ccmc.gsfc.nasa.gov/ modelweb / models/nrlmsise00.php.tion.

Author contributions

YL performed the modeling calculations and writing. HL and ZZX provided theoretical guidance, JW,XBL,CLand CXY participated in the discussion and given valuable comments.

Competing interests

The contact author has declared that none of the authors has any competing interests.

Acknowledgments

This work supported by “the Fundamental Research Funds for the Central Universities” (Grant No. HIT.OCEF.2022036）

References

Barr, R. and Stubbe, P.: ELF and VLF wave generation by HF heating: A comparison of AM and CW techniques, Journal of Atmospheric and Solar-Terrestrial Physics, 59, 2265-2279, https://doi.org/1016/s1364-6826(96)00121-6, 1997.

Belyaev, P. P., Kotik, D. S., Mityakov, S. N., Polyakov, S. V., Rapoport, V. O., and Trakhtengerts, V. Y.: Generation of electromagnetic signals at combination frequencies in the ionosphere, Radiophys. Quantum Electron. 30:2, 189-206, https://doi.org/1007/bf01034491, 1987.

Chen, F. F.: Introduction to plasma physics, Springer Science & Business Media, ISBN:1475704593, 2012.

Cohen, M. B., Inan, U. S., and Golkowski, M. A.: Geometric modulation: A more effective method of steerable ELF/VLF wave generation with continuous HF heating of the lower ionosphere, Geophysical Research Letters, 35, https://doi.org/1029/2008gl034061, 2008.

Cohen, M. B., Inan, U. S., and Golkowski, M. A.: Reply to comment by R. C. Moore and M. T. Rietveld on "Geometric modulation: A more effective method of steerable ELF/VLF wave generation with continuous HF heating of the lower ionosphere", Geophysical Research Letters, 36, https://doi.org/1029/2008gl036519, 2009.

Eliasson, B., Chang, C. L., and Papadopoulos, K.: Generation of ELF and ULF electromagnetic waves by modulated heating of the ionospheric F2 region, J. Geophys. Res-Space Phys., 117, 22, https://doi.org/1029/2012ja017935, 2012.

Ganguly, S.: Experimental observation of ultra-low-frequency waves generated in the ionosphere, Nature, 320, 511-513, https://doi.org/1038/320511b0, 1986.

Getmantsev, G., Zuikov, N., and Kotik, D.: Combination frequencies in the interaction between high-power short-wave radiation and ionospheric plasma, ZhETF Pisma Redaktsiiu, 20, 229-232, 1974.

Gurevich, A.: Nonlinear phenomena in the ionosphere, Springer Science & Business Media,ISBN: 3642876498,2012.

Gustavsson, B., Rietveld, M. T., Ivchenko, N. V., and Kosch, M. J.: Rise and fall of electron temperatures: Ohmic heating of ionospheric electrons from underdense HF radio wave pumping, J. Geophys. Res-Space Phys., 115, https://doi.org/1029/2010ja015873, 2010.

Banks, P. M. and Kockarts, G.: Aeronomy, Academic Press, https://doi.org/10.1016/B978-0-12-077802-7.50012-9, 1973.

Kotik, D. S., Ryabov, A. V., Ermakova, E. N., and Pershin, A. V.: Dependence of Characteristics of SURA Induced Artificial ULF/VLF Signals on Geomagnetic Activity, Earth Moon and Planets, 116, 79-88, https://doi.org/1007/s11038-015-9465-y, 2015.

Kotik, D. S., Ryabov, A. V., Ermakova, E. N., Pershin, A. V., Ivanov, V. N., and Esin, V. P.: Properties of the ULF/VLF Signals Generated by the Sura Facility in the Upper Ionosphere, Radiophysics and Quantum Electronics, 56, 344-354, https://doi.org/1007/s11141-013-9438-9, 2013.

Kuo, S., Snyder, A., and Chang, C.-L.: Electrojet-independent ionospheric extremely low frequency/very low frequency wave generation by powerful high frequency waves, Physics of Plasmas, 17, https://doi.org/1063/1.3476290, 2010.

Kuo, S., Snyder, A., Kossey, P., Chang, C.-L., and Labenski, J.: Beating HF waves to generate VLF waves in the ionosphere, J. Geophys. Res-Space Phys., 117, https://doi.org/1029/2011ja017076, 2012.

Kuo, S., Snyder, A., Kossey, P., Chang, C. L., and Labenski, J.: VLF wave generation by beating of two HF waves in the ionosphere, Geophysical Research Letters, 38, https://doi.org/1029/2011GL047514, 2011.

Lofas, H., Ivchenko, N., Gustavsson, B., Leyser, T. B., and Rietveld, M. T.: F-region electron heating by X-mode radiowaves in underdense conditions, Annales Geophysicae, 27, 2585-2592, https://doi.org/10.5194/angeo-27-2585-2009,2009.

Lysak, R. L.: Propagation of Alfvén waves through the ionosphere, Physics and Chemistry of the Earth, 22, 757-766, doi.org/10.1016/S0079-1946(97)00208-5, 1997.

Milikh, G. M. and Papadopoulos, K.: Enhanced ionospheric ELF/VLF generation efficiency by multiple timescale modulated heating, Geophys Res Lett, 34, https://doi.org/1029/2007gl031518, 2007.

Moore, R. C.: ELF/VLF wave generation by modulated HF heating of the auroral electrojet, PhD thesis, Stanford University, 2007.

Papadopoulos, K., Chang, C. L., Labenski, J., and Wallace, T.: First demonstration of HF-driven ionospheric currents, Geophysical Research Letters, 38, L12103, https://doi.org/1029/2011gl049263, 2011a.

Papadopoulos, K., Chang, C. L., Vitello, P., and Drobot, A.: ON THE EFFICIENCY OF IONOSPHERIC ELF GENERATION, Radio Science, 25, 1311-1320, https://doi.org/1029/RS025i006p01311, 1990.

Papadopoulos, K., Gumerov, N. A., Shao, X., Doxas, I., and Chang, C. L.: HF-driven currents in the polar ionosphere, Geophysical Research Letters, 38, L20107, https://doi.org/1029/2011gl047368, 2011b.

Rietveld, M. T., Mauelshagen, H.-P., Stubbe, P., Kopka, H., and Nielsen, E.: The characteristics of ionospheric heating-produced ELF/VLF waves over 32 hours, Journal of Geophysical Research: Space Physics, 92, 8707-8722, doi.org/10.1029/JA092iA08p08707, 1987.

Schunk, R. and Nagy, A.: Ionospheres: physics, plasma physics, and chemistry, Cambridge university press,ISBN: 0521877067,2009.

Sharma, A. S., Eliasson, B., Shao, X., and Papadopoulos, K.: Generation of ELF waves during HF heating of the ionosphere at midlatitudes, Radio Science, 51, 962-971, https://doi.org/1002/2016rs005953, 2016.

Shoucri, M. M., Morales, G., and Maggs, J.: Ohmic heating of the polar F region by HF pulses, Journal of Geophysical Research: Space Physics, 89, 2907-2917, https://doi.org/10.1029/JA089iA05p02907, 1984.

Stubbe, P. and Kopka, H.: Modulation of the polar electrojet by powerful HF waves, Journal of Geophysical Research, 82, 2319-2325, https://doi.org/1029/JA082i016p02319, 1977.

Stubbe, P., Kopka, H., and Dowden, R. L.: Generation of ELF and VLF waves by polar electrojet modulation: Experimental results, Journal of Geophysical Research, 86, https://doi.org/1029/JA086iA11p09073, 1981.

Willis, J. W. and Davis, J. R.: Radio frequency heating effects on electron density in the lower E region, Journal of Geophysical Research (1896-1977), 78, 5710-5717, https://doi.org/1029/JA078i025p05710, 1973.